Minerals Engineering 237 (2026) 109990

Contents lists available at ScienceDirect

Minerals Engineering

journal homepage: www.elsevier.com/locate/mineng

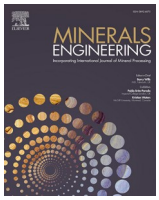

Selective leaching of Cu and Co from stratiform sediment-hosted copper ore using deep eutectic solvents

Rupert Heathcote [a,*], William Nash [b,a], Arthur Graf [c], Karen A. Hudson-Edwards [a], Rich Crane [a]

[a] Camborne School of Mines, University of Exeter, UK
[b] Helmholtz-Zentrum Dresden-Rossendorf, Saxony, Germany
[c] National Research Facility for X-ray Photoelectron Spectroscopy, School of Chemistry, Cardiff University, UK

ARTICLE INFO

Keywords:
Cobalt
Copper
Deep eutectic solvent
Leaching

ABSTRACT

Hydrometallurgical processing of sediment-hosted stratiform Cu ores traditionally relies on strong, often toxic mineral acids, with a primary focus on Cu recovery. Cobalt, an important but frequently overlooked byproduct, is typically recovered with poor efficiency (e.g., ~45 %). To address this knowledge gap, we investigated the simultaneous leaching of Cu and Co from a Cu ore from the Central African Copperbelt using oxalic, formic, and lactic acid-based choline chloride (ChCl) deep eutectic solvents (DESs). Results were compared with conventional leaching using sulfuric acid (10 g/L), both with and without ferrous sulfate (1.5 g/L). Across the temperature (20–80 °C) and time (1–90 h) ranges studied, all DES formulations achieved leaching efficiencies comparable to those of sulfuric acid. Choline chloride–lactic acid (ChCl:LA) exhibited the best overall performance, yielding higher selectivity for Cu and Co. This was most pronounced at 20 °C, where, after 90 h, 94 % and 85 % of Cu and Co were respectively leached, but only 5 % of the Fe was dissolved, compared to 96 %, 76 % and 9 % recorded for sulfuric acid. These findings highlight the potential of DESs, particularly those composed of hydrogen bond donors with chelating and reducing properties, such as ChCl:LA, as highly promising alternatives for Cu and Co leaching from stratiform sediment-hosted Cu ores.

1. Introduction

Critical metals such as Cu and Co are essential elements in modern technologies and for the global transition towards net-zero carbon emissions. As nations continue to upscale their modern and clean energy technology provision, demand for these metals is surging, with Cu and Co consumption expected to increase by 46 % and 111 %, respectively, by 2040 (IEA, 2024). While major progress has been made in recent years in enhancing the efficiency of Cu and Co mining and mineral processing, this expansion is poised to create substantial challenges associated with extracting these metals without incurring prohibitively high socioeconomic and environmental costs (Valenta et al., 2019). As a result, there is now an unprecedented need to develop innovative technologies that improve the extraction of metals from ores.

Stratiform sediment-hosted (SSH) Cu ores constitute 25 % and 76 % of the world's Cu and Co production, respectively, and are second only to porphyry Cu ores in terms of economic importance (Dehaine et al., 2021; Misra, 2000; USGS, 2025). Copper is typically extracted from stratiform Cu ore using a sulfuric acid hydrometallurgical treatment, which is reliable and relatively low-cost, but typically exhibits relatively poor Cu leaching efficiency of approximately 75 % (Shengo et al., 2019). Moreover, it is also often not normally adapted for the co-leaching of Co, with recoveries of approximately 40 % (Dehaine et al., 2021; Fisher, 2011). Consequently, substantial amounts of Cu and Co are sent to tailings, resulting in both economic losses and severe environmental (Fisher, 2011; Kalenga, 2013; Muimba-Kankolongo et al., 2022) and human health impacts (Brusselen et al., 2020; Kayembe-Kitenge et al., 2019). For example, in the Democratic Republic of Congo (DRC) alone, there are several hundred million tonnes of Cu-Co tailings currently stockpiled, with Cu and Co concentrations reportedly as high as approximately 1 wt% and 0.1 wt%, respectively (Lutandula and Maloba, 2013).

Sulfuric acid is a strong acid with a tendency for non-selective leaching, due to its reactivity with gangue minerals, leading to several undesirable outcomes such as the excessive generation of mixed-metal leachates, consumption of carbonates, and the transformation of

* Corresponding author.
E-mail address: rrjh201@exeter.ac.uk (R. Heathcote).

https://doi.org/10.1016/j.mineng.2025.109990
Received 12 September 2025; Received in revised form 26 November 2025; Accepted 30 November 2025
Available online 13 December 2025

silicates into gel (Tanda et al., 2017). It also commonly produces insoluble metal salts (e.g. calcium sulfate), which can lead to substantial scaling within hydrometallurgical equipment (Binnemans and Jones, 2023a; Crundwell et al., 2020). Additionally, in Cu electrometallurgy, the limited solubility of $CuSO_4{\cdot}5H_2O$ in sulfuric acid solutions can restrict the maximum Cu concentration in the advanced electrolyte, thereby negatively impacting the efficiency of both Cu electrowinning and electrorefining (Schlesinger et al., 2011). There is consequently a pressing demand for the development of new metallurgical processes which both improve leaching efficiencies and enhance environmental compatibility, safety, and sustainability.

Green chemistry is a principle that aims to reduce the use and production of hazardous substances in chemical processes while also minimising energy consumption and increasing the use of renewable sources (Binnemans and Jones, 2023b, 2017; Clarke et al., 2018). Within this field, deep eutectic solvents (DESs) have emerged as promising green solvents for the extraction of Cu and Co from geological materials owing to their high metal solubility, low volatility, customisable properties, affordability, and potential environmental compatibility (Abranches and Coutinho, 2023; Bystrzanowska and Tobiszewski, 2021; Hansen et al., 2021; Radošević et al., 2015; Sharma and Lee, 2024; Smith et al., 2014). Among these, Type III DESs, which consist of a quaternary ammonium salt (e.g., ChCl) and a hydrogen bond donor (e.g., carboxylic acid), offer several advantages for metal extraction. These include a high capacity to dissolve metals from a variety of transition metal-bearing minerals, including oxides (Abbott et al., 2005), chlorides (Abbott et al., 2003), sulfides and tellurides (Carlesi et al., 2022; Jenkin et al., 2016).

Despite such interest, the application of DESs for the simultaneous leaching of Cu and Co from both natural and engineered materials remains largely unexplored. Most investigations to date have investigated the recovery of these metals from secondary sources, such as spent lithium-ion and Ni batteries, used NdFeB magnets, printed circuit boards, and synthetic metal oxides (Landa-Castro et al., 2020; Mishra et al., 2024; Riaño et al., 2017; Tran et al., 2019; Wang et al., 2020). In addition, a limited number of studies have examined the leaching of Cu from its parent minerals (Aragón-Tobar et al., 2024) and sulfide ores (Anggara et al., 2019; Carlesi et al., 2022). However, the application of DESs for the simultaneous leaching of Cu and Co from natural mixed ores remains untested.

Whilst some insight into their behaviour has been provided by Oke et al. (2025), who tested DES-water mixtures (30 wt% water) for the leaching of Cu and Co at elevated temperature (30–75 °C) from ore taken from the DRC. Yet, the well-documented differences in behaviour between aqueous and pure DESs limit the applicability of these results for understanding DES leaching mechanisms (Abbott and Frisch, 2013). Furthermore, the study measured only Cu and Co in the leachates, leaving significant knowledge gaps regarding the interactions of DESs with other metal constituents and gangue minerals—factors critical to understanding overall leaching performance and selectivity.

To address these gaps, the present study is the first-ever to investigate the application of pure ChCl-based DES formulations (using oxalic, lactic, and formic acids) for the leaching of Cu and Co from a naturally occurring, mineralogically complex mixed oxide ore from the DRC. As one of the world's largest producers of Cu and Co, the DRC faces significant environmental and social challenges in ensuring the sustainable extraction of these metals (RAID, 2024; USGS, 2025). By examining DES leaching across a range of temperatures and contact times—including, for the first time, under ambient (20 °C) conditions—this study provides a comprehensive evaluation of DES performance and benchmarks it against a conventionally applied hydrometallurgical process. Importantly, we also investigate DES selectivity, kinetics, and interactions with co-occurring gangue minerals to assess their viability as environmentally sustainable alternatives for extracting Cu and Co from oxide ores.

2. Materials and methods

2.1. Site description and sample collection

The sample used herein was a blend of stockpiled stratiform sediment-hosted Cu ore from the Katanga Province of the DRC, consisting of Cu-Co sulfides and oxides hosted by Neoproterozoic metasedimentary rocks (Shengo et al., 2019), which have undergone supergene enrichment (Decrée et al., 2010; Mambwe et al., 2022). Prior to the leaching experiments, a subsample of approximately 1 kg was riffle-split and then ground using a TEMA mill to a D_{80} (screen opening in microns through which 80 % material passes) of 40.4 μm ± 1.3 to ensure homogeneity between samples and provide a representative feedstock for the leaching experiments.

2.2. Chemicals and standards

Choline chloride (99 %), DL-lactic acid (85 %), formic acid (98 %), aluminium sulfate octadecahydrate (100 %), and iron(II) sulfate heptahydrate (98 %) were purchased from Thermo Scientific Acros. Oxalic acid dihydrate (≥99 %), was purchased from Sigma Aldrich. Ammonium acetate (≥99 %), magnesium sulfate heptahydrate (≥99 %), acetic acid glacial (≥99.7 %), hydroxylamine hydrochloride (>99 %), hydrogen peroxide (30 %), nitric acid (68–70 % certified for analysis), and sulfuric acid (98 %) were purchased from Fisher Scientific. Reagecon's 19-element standard (REICPCAL19L) was used for calibration of the ICP–OES. Leachate samples and calibration solutions were diluted using 2.5 % nitric acid, which was synthesised by diluting analytical-grade nitric acid with ultrapure deionised water (Milli-Q, 18.2 MΩ cm). Calibration curves were made using solutions of 0.01, 0.1, 1, 5, 10, and 25 ppm of the multi-element standard.

Three types of DES were synthesised: choline chloride–lactic acid (ChCl:LA), choline chloride–formic acid (ChCl:FA) and choline chloride–oxalic acid (ChCl:OA). Synthesis followed the methods of Rodriguez et al. (2019) and Abbott et al. (2003). The molar ratios were 1:2 for ChCl:LA and ChCl:FA, and 1:1 for ChCl:OA. The hydrogen bond donor (HBD) compounds and ChCl were mixed under constant stirring (100 rpm) for 6 h at 20 °C for ChCl:LA and ChCl:FA, and at 50 °C for ChCl:OA synthesis, which required a higher temperature to form a eutectic mixture. These temperatures were chosen as the lowest feasible to minimise esterification while still allowing the DES to form within this timescale (Thompson et al., 2022). Once a homogeneous and clear liquid was observed, the resulting eutectic mixture was removed from the hotplate and allowed to cool to ambient temperature before further use.

The 'sulfuric acid' leaching solution was prepared by dissolving 1.6 g of $Al_2(SO_4)_3{\cdot}18H_2O$, 1.5 g of $MgSO_4{\cdot}7H_2O$, and 10 g H_2SO_4 in 1 L of Milli-Q water (18.2 MΩ cm). Aluminium and Mg reagents were added to mimic the presence of these metals in natural waters. The 'ferrous sulfuric acid' leaching solution was prepared by adding 1.5 g/L $FeSO_4{\cdot}7H_2O$ into an aliquot of the sulfuric acid solution.

2.3. Sample characterisation

The powdered Cu ore feedstock was divided into three 10 g aliquots using a riffle splitter and submitted to a commercial analytical laboratory (ALS Global, Loughrea, Co. Galway, Ireland) for digestion and geochemical analysis. Elemental concentrations, including major and trace elements, were measured using inductively coupled plasma – mass spectroscopy (ICP–MS) following a four-acid digestion (perchloric, nitric, hydrofluoric, and hydrochloric) of 0.02 g of the powdered ore, in accordance with ALS method ME-MS61™. Copper concentrations in the sample exceeded the over-range threshold and were reanalysed using the ore grade Inductively Coupled Plasma – Atomic Emission Spectroscopy (ICP–AES) method (ALS method: Cu-OG62™). All analyses were performed in triplicate, and matrix-matched certified reference materials (OREAS-45f, OREAS 605b, CD-1) were used to evaluate the

accuracy of the digestion process.

Sequential extractions were undertaken to investigate the geochemical speciation of metals within the ore, using the modified BCR (Community Bureau of Reference) sequential extraction procedure (Rauret et al., 1999). This was applied to both the as-received (without milling) and milled ore to also yield insight into their liberation and associated leachability. In brief, 0.5 g of each dry sample was exposed to 0.11 M acetic acid, 0.5 M hydroxylamine hydrochloride, 8.8 M hydrogen peroxide combined with 1.0 M ammonium acetate, and finally four-acid digestion, which are respectively attributed to dissolve the exchangeable, reducible, oxidisable, and residual fractions. Extractants were diluted in 2.5 % HNO_3 and analysed using Inductively Coupled Plasma – Optical Emission Spectroscopy (ICP–OES). All experiments were performed in triplicate.

The mineralogy of the sample was characterised using X-ray diffraction (XRD) and automated mineralogy using a QEMSCAN® (Quantitative Evaluation of Minerals by Scanning Electron Microscopy). For XRD analysis, the samples were milled to a fine powder before being mounted into a Bruker D6 Phaser. XRD intensities were measured across a 2θ range of 2–70° using a step size of 0.01°, with a counting time of 0.1 s per step. For QEMSCAN® analysis, the as-received sample was mounted in a 30 mm diameter epoxy resin block. The upper face of the block was polished to a 1 μm finish using diamond paste and coated with a 25 nm layer of carbon before analysis. Samples were analysed using QEMSCAN® 4300 on a Zeiss Evo 50 system using the FieldImage mode at a pixel spacing resolution of 10 μm, which generated 2,934,287 analysis points. An 'area%' calculation (total number of pixels of a mineral as a percentage of the total number of pixels in the sample) was used to provide an estimate of the modal mineralogy of the Cu ore sample. Analyses were carried out using a 20nA electron beam accelerated to 15 kV and focused to a diameter of 1 μm. Quantitative mineral composition data were obtained using a CAMECA SX-5 FE electron-probe microanalysis (EPMA) with an unregulated beam at 20nA for cupro-asbolane and 10nA for carbonate phases, and 15 kV acceleration. Analytical volumes were 2 μm^3. Counting times were $\geq$ 30 s for peaks, 15 s for backgrounds, and 60 s for trace elements. Total Mn and Co were calculated as their tetravalent and trivalent forms, respectively. The ZAF correction method was applied to the data, and water content was calculated by difference and compared to predicted values from other hydrated minerals.

The powdered ore and residues resulting from 1 h, 6 h, and 24 h leaching experiments with ChCl:OA, ChCl:LA, and ChCl:FA, were analysed using X-ray photoelectron spectroscopy (XPS) to determine leaching reaction mechanisms. Prior to analysis, the residues were rinsed three times with Milli-Q water (18.2 MΩ cm) and dried in an oven overnight at 38 °C. XPS data were acquired using a Kratos Axis SUPRA with monochromated Al kα (1486.69 eV) X-rays at 15 mA emission and 12 kV high tension (180 W) and a spot size/analysis area of 700 x 300 μm. The instrument was calibrated to gold metal Au 4f (83.95 eV) and dispersion adjusted to give a binding energy (BE) of 932.6 eV for the Cu $2p_{3/2}$ line of metallic Cu. Ag $3d_{5/2}$ line full width at half maximum (FWHM) at 10 eV pass energy was 0.544 eV. Source resolution for monochromatic Al Kα X-rays was ~ 0.3 eV. The instrumental resolution was determined to be 0.29 eV at 10 eV pass energy using the Fermi edge of the valence band for metallic silver with a charge compensation system on < 1.33 eV FWHM on polytetrafluoroethylene (PTFE). High-resolution spectra were obtained using a pass energy of 20 eV, a step size of 0.1 eV, and a sweep time of 60 s, resulting in a line width of 0.696 eV for the Au $4f_{7/2}$. Survey spectra were obtained using a pass energy of 160 eV. Charge neutralisation was achieved using an electron flood gun with filament current = 0.4 A, charge balance = 2 V, filament bias = 4.2 V. Successful neutralisation was adjusted by analysing the C 1 s region, wherein sharp peaks with no lower BE structure were obtained. Spectra were charge-corrected to the main line of the carbon 1 s spectrum (adventitious carbon), set to 284.8 eV. All data were recorded at a base pressure below 9 x 10^{-9} Torr and a room temperature of 294 K. The data were analysed using CasaXPS v2.3.19PR1.0. Peaks were fit with a Shirley background before component analysis.

2.4. Leaching experiments

Leaching experiments were conducted by adding 0.25 g of milled Cu ore to a 28 mL tall-form glass vial along with a PTFE magnetic stir bar. Following this, 5.0 g of solvent (*i.e.* DES or H_2SO_4) was added, resulting in a 1:20 solid:liquid ratio. This ratio was selected to ensure a sufficient excess of DES so that external mass transfer was not the rate-limiting step, and also for comparison with previous DES leaching research where such a high excess of the solvent has been applied. The vial was then secured beneath a borosilicate glass condenser coil and lowered into a 250 mL oil bath on a hotplate. The stirring speed was set to 400 rpm. Leaching tests were performed at 20 °C, 40 °C, 60 °C, and 80 °C, and monitored using FEP-insulated Type-K thermocouples. These were fed through the condenser directly into the glass vial. Data were collected every second using a Thermosense 4 Channel Thermocouple Data. After leaching, the supernatant liquid was extracted using a pipette, transferred into a 50 mL Falcon tube and then centrifuged at 3000 rpm for 15 min. The supernatant was extracted from the residue using a 20 mL sterile syringe and passed through using a 0.45 μm nylon syringe filter. The solution was then diluted with 2.5 % HNO_3 and analysed using ICP–OES to determine its metal concentrations. All leaching experiments were executed in triplicate.

Conventional Cu and Co leaching from SSH ore from the DRC is typically undertaken using sulfuric acid or ferrous sulfuric acid (Shengo et al., 2019). To compare our results with this industry-standard process, low temperature (20 °C) leaching tests were also undertaken using 10 g/L solutions of H_2SO_4 and H_2SO_4 with (1.5 g/L) $FeSO_4$, for a duration of 1–90 h, under the same conditions applied in the DES leaching tests.

3. Results and Discussion

3.1. Geochemical and mineralogical characterisation of the Cu ore

The SSH Cu ore sample had a total Cu content of 2.54 wt% (Table 1), similar to average Cu ore grades (~2.63 wt%) recorded for the Central African Copperbelt (CAC) (Ndonfack et al., 2024), but a lower concentration of Co (0.17 wt%) than typically measured in high-grade Co deposits (average 0.58 wt%) in the region (Dehaine et al., 2021). Iron (5.20 wt%) and Al (5.62 wt%) were also abundant, indicative of silicate and oxide minerals in the matrix. Concentrations of Mn (2470 ppm) and Ca (1770 ppm) suggested the presence of plagioclase or carbonate and Mn-bearing phases. Elevated ecotoxic element concentrations of As (394 ppm), Zn (657 ppm), and Pb (458 ppm) presage potential hazards to the environment during the processing of these ores and waste storage.

Sequential extraction results indicate that in the milled sample, Cu was primarily exchangeable (46 %) and reducible (26 %), with minor oxidizable (1 %) and residual fractions (28 %) (Fig. 1). In contrast, Co was hosted mainly in the reducible fraction (66 %), with only a small exchangeable fraction (2 %). This suggested that effective leaching of Cu and Co simultaneously would likely require a reducing agent in acidic media. However, given that Mn and Fe are also susceptible to leaching under reducing conditions (80 % and 2 % of these metals occurred in the reducible phase, respectively), such an approach would likely be relatively non-selective (Fig. 1).

XPS was used to examine the surface composition of the ore sample. Cobalt exhibited a $2p_{3/2}$ peak with a BE centred at 779.5 eV. The shape of the spectrum and the observed multiplet splitting were consistent with Co_3O_4 (Fig. S2), suggesting that Co was present in both trivalent and divalent forms, which corroborates the mineralogical analysis (Table 2; Table 3). Manganese was found in Mn_2O_3 form, confirming trivalent Mn on the mineral surfaces. The Fe 2p spectra indicated that Fe was present in a trivalent state. The Cu 2p spectra showed a mixed Cu

Table 1
Geochemical composition of the Cu ore by total digestion of the sample followed by Inductively Coupled Plasma – Atomic Emission Spectroscopy / Mass Spectroscopy (ICP–AES/MS) analysis.

Element	wt. %	Element	ppm	Element	ppm	Element	ppm	Element	ppm
Al	5.62	Ag	4.96	Hf	4.23	Sb	98.8	W	19.4
Ca	0.18	As	394	In	1.63	Sc	24.7	Y	29.0
Co	0.17	Ba	490	La	197	Se	7.67	Zn	657
Cu	2.54	Be	4.31	Li	65.2	Sn	7.03	Zr	170
Fe	5.20	Bi	1.59	Mo	13.2	Sr	24.0		
K	1.99	Cd	1.16	Nb	19.9	Ta	1.28		
Mg	3.17	Ce	164	Ni	176	Te	0.11		
Mn	0.25	Cr	201	P	2070	Th	10.0		
Na	0.03	Cs	0.66	Pb	458	Tl	0.28		
S	0.04	Ga	50.4	Rb	64.5	U	18.3		
Ti	0.50	Ge	0.38	Re	0.002	V	454		

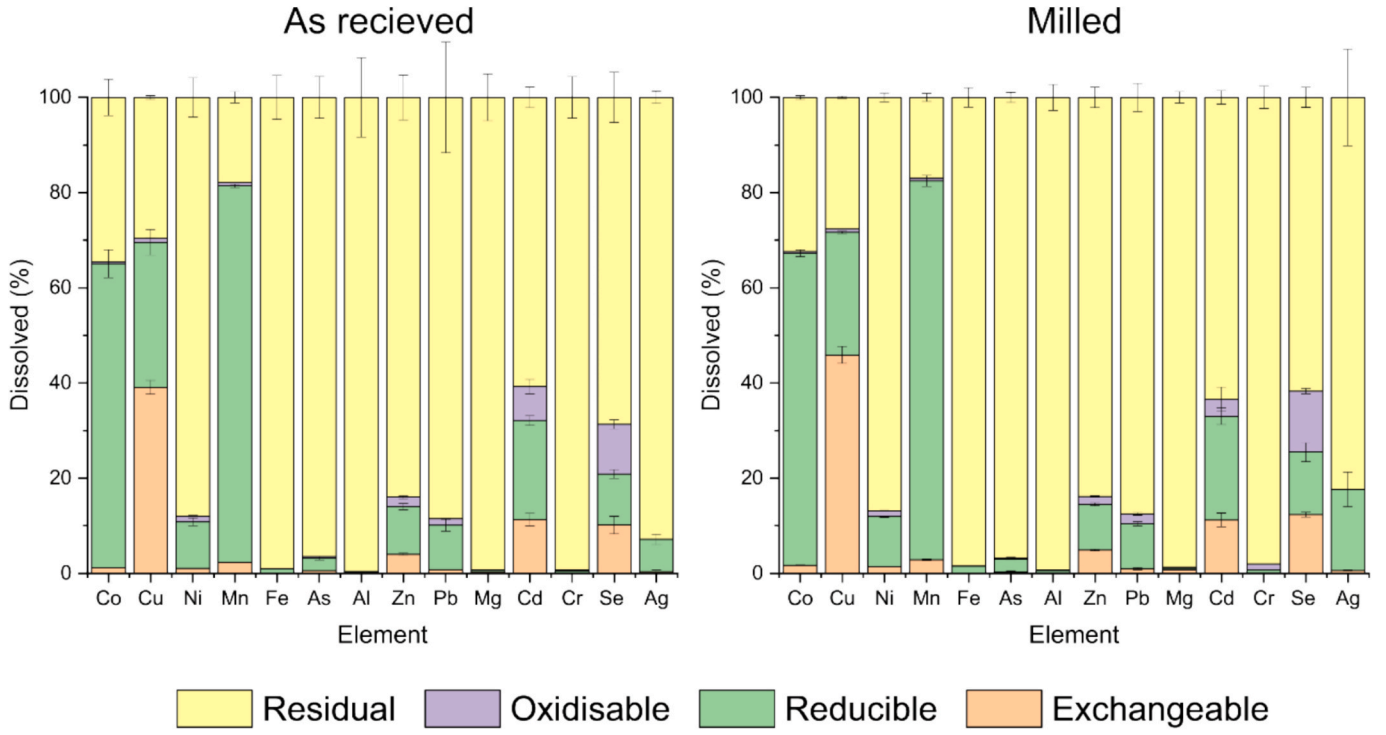

Fig. 1. Proportions of metals/metalloid in exchangeable, reducible, oxidisable, and residual phases as determined by the modified BCR (Community Bureau of Reference) sequential extraction procedure, for the as received and milled Cu ore. Each bar represents the mean normalised percent of triplicate samples, and error bars are ± 1 standard deviation.

(I)/Cu(II) surface composition, with a ratio of approximately 2:1.

Analysis of the sample using XRD and QEMSCAN® (Table 2, Fig. S1) showed that quartz, micas, and chlorite were primary mineral phases, along with a notable presence of Cu- and Co-bearing minerals (accounting for 6.2 % of the analysed area). Malachite/azurite was the most abundant Cu mineral, followed by chrysocolla and pseudomalachite. Cobalt minerals were less abundant than Cu minerals; cupro-asbolane was the most abundant in the sample, followed by a low abundance of kolwezite and heterogenite. Malachite/azurite and pseudomalachite exhibited a high degree of liberation (17.2 %) and an association with other relatively soluble Cu-Co minerals, suggesting that they are physically amenable to leaching (i.e. not bound to or within insoluble minerals, which could inhibit their exposure to a solvent). In contrast, heterogenite and chalcopyrite had lower degrees of liberation (12 %, respectively). Cupro-asbolane and chrysocolla exhibited a notable association with mica and clay minerals (23.8 %), which may also negatively influence Cu and Co dissolution kinetics, given that clays are generally poorly soluble under acidic and reducing conditions (Terry, 1983).

Chemical microanalysis of the major Cu and Co minerals revealed malachite/azurite as the most Cu-enriched mineral (71.7 wt% CuO), and heterogenite and kolwezite were the most Co-rich minerals, averaging 48.7 wt% and 44.8 wt% CoO, respectively (Table 3). Cupro-asbolane contained relatively high concentrations of several metals, including CuO (14.5 wt%), CoO (7.74 wt%), MnO_2 (29.4 wt%), and Fe_2O_3 (13.9 wt %).

The multi-metal composition of cupro-asbolane suggests that leaching of Cu and Co could result in co-leaching of Mn and Fe (Table 3). This is supported by the sequential extraction results (Fig. 1), which show that considerable proportions of Cu, Co, Mn, and Fe were hosted within minerals which are amenable to reductive dissolution. Similarly, the other Co-bearing minerals (such as kolwezite and heterogenite) contained Fe_2O_3, suggesting that their dissolution may lead to the co-dissolution of Fe. Additionally, these minerals contained relatively high concentrations of CuO (12.6 wt% and 4.95 wt%, respectively). This suggests that, to achieve maximum Cu leaching efficiencies, the dissolution of Co-bearing minerals is also necessary, but this could introduce other impurities into the leachate.

Table 2
Mineralogy of the Cu ore as determined using X-ray diffraction (XRD) and QEMSCAN® (Quantitative Evaluation of Minerals by Scanning Electron Microscopy). The degree of liberation is a proxy based on area% of the free boundaries of grains. The association with 'valuable' minerals reflects mineral associations with CuCo minerals.

Mineral	Formula	XRD	QEMSCAN abundance (area %)	Degree of liberation (%)	Association with 'valuable' minerals (%)
Quartz	SiO_2	X	39	30	3.1
Plagioclase / K-feldspar	$(Na,Ca)(Si,Al)_4O_8$ / $KAlSi_3O_8$		13	22	1.7
Calcite / dolomite / ankerite	$CaCO_3$ / $CaMg(CO_3)_2$ / $Ca(Fe^{2+},Mg,Mn)(CO_3)_2$		0.6	36	1.9
Muscovite	$KAl_2(Si_3Al)O_{10}(OH,F)_2$	X	7.4	15	1.6
Biotite	$K(Mg,Fe^{2+})_3AlSi_3O_{10}(OH,F)_2$		5.2	18	4.1
Phlogopite	$KMg_3(Si_3Al)O_{10}(F,OH)_2$		4.3	31	2.8
Chlorite / clinochlore	$(Mg,Fe^{3+})_5Al(Si_3Al)O_{10}(OH)_8$	X	15	38	4.7
Arsenides and other sulfides	(Fe,Cu,Co,Ni)(As,S)		< 0.1	30	16
Goethite	$Fe^{3+}O(OH)$	X	4.4	25	20
Cupro-asbolane	$(Ni,Co,Cu)_xMn^{4+}(O,OH)_4{\cdot}nH_2O$		0.7	28	22
Kolwezite	$(Cu,Co)_2(CO_3)(OH)_2$		0.1	21	43
Heterogenite	CoO(OH)		< 0.1	12	20
Chrysocolla	$(Cu,Al)_2H_2Si_2O_5(OH)_4{\cdot}n(H_2O)$		1.8	22	25
Malachite / azurite	$Cu_2(CO_3)(OH)_2$ / $Cu_3(CO_3)_2(OH)_2$	X	2.6	17	37
Pseudomalachite	$Cu_5(PO_4)_2(OH)_4$		0.7	28	39
Chalcocite	Cu_2S		0.2	34	31
Chalcopyrite	$CuFeS_2$		0.1	13	39
Cu-oxide	CuO		< 0.1	2.4	85

X: mineral identified using XRD.

Table 3
Selected oxide concentrations present within Cu- and Co-bearing minerals in the Cu ore as determined by electron-probe microanalysis (EMPA) (b. d. = below detection limit).

Mineral	CuO (wt. %)	CoO (wt. %)	SiO_2 (wt. %)	Al_2O_3 (wt. %)	Fe_2O_3 (wt. %)	MnO_2 (wt. %)
Cupro-asbolane	14.5 ± 3.3	7.74 ± 2.6	2.36 ± 1.5	2.12 ± 0.9	13.9 ± 11	29.4 ± 11
Kolwezite	12.6 ± 4.3	44.8 ± 6.8	2.12 ± 0.6	0.89 ± 0.3	13.4 ± 7	4.05 ± 1.4
Heterogenite	4.95 ± 0.7	48.7 ± 12	1.19 ± 0.6	1.04 ± 0.8	14.0 ± 9	3.43 ± 1.8
Malachite / azurite	71.7 ± 0.3	b. d.	0.05 ± 0.05	0.09 ± 0.08	0.07 ± 0.04	
Pseudomalachite	66.7 ± 2.1	b. d.	0.13 ± 0.1	b. d.	0.06 ± 0.02	
Chrysocolla	9.15 ± 0.8	0.22 ± 0.03	32.8 ± 1	16.8 ± 0.4	2.84 ± 0.2	

3.2. Leaching experiments

Experimentally measured leaching efficiencies—defined as the ratio of metal dissolved by the solvent to metal initially present in the Cu ore sample—are shown in Fig. 2 as functions of temperature (Fig. 2a–c) and time (Fig. 2d–f).

For all three DESs tested, Cu leaching efficiencies were 0.75 or greater after 24 h of leaching at temperatures above 20 °C, and consistently exceeded 0.9 at temperatures above 40 °C. Cobalt leaching efficiencies were somewhat lower, but nonetheless consistently greater than 0.65 at 40 °C or higher, with 0.83–0.95 recorded at 80 °C. For every metal-DES combination, leaching efficiency exhibited a positive correlation with temperature, except for Ni in ChCl:OA.

In most cases, leaching efficiencies were higher for Cu, Co and Mn than for Fe, Ni and As. This is attributed to the clear differences in extractability of these elements from the ore using acidic and chemical reducing conditions (Fig. 1). Such contrasting behaviour between these two groups of metals is most pronounced when leaching is undertaken at low temperature (Fig. 2a–c). Above 60 °C, this distinction is evident only for ChCl:FA and ChCl:LA, which display very similar leaching profiles; however, ChCl:LA generally achieved higher efficiencies for the target metals.

The time-series plots (Fig. 2d–f) indicate that at 20 °C, ChCl:FA and ChCl:LA established equilibria with the Cu-, As- and Fe-bearing phases relatively quickly (~24 h), but not with the Co–, Mn- and Ni-bearing phases, even after 90 h of leaching. ChCl:OA exhibited almost the opposite behaviour, with rapid (>12 h) equilibration with Co–, Mn- and Ni-bearing phases, but no equilibrium with As- and Fe-bearing phases. High yields were also quickly established for Cu, indicating a similar proficiency for this system. However, the Cu yields for ChCl:OA subsequently decreased, suggesting that Cu^{2+} ions in the DES precipitated or were replaced by another ion, such as Fe.

The similar leaching behaviour between Mn and Co was consistent with the QEMSCAN® and EPMA data (Table 2; Table 3), which show that both metals were dominantly hosted by cupro-asbolane; dissolution of this mineral simultaneously liberated both metals. The time-series plots (Fig. 2d–f) suggest that ChCl:OA dissolved this mineral substantially faster than ChCl:FA and ChCl:LA, possibly due to it exhibiting two carboxyl groups, whilst ChCl:FA and ChCl:LA are monocarboxylic.

A much smaller portion of Cu was hosted by pseudomalachite and chrysocolla. These minerals may have been responsible for the increased Cu yield with temperature.

Iron leaching was typically low at 20 °C, with ChCl:FA and ChCl:LA achieving a leaching efficiency less than 0.05, whilst ChCl:OA was less than 0.2, which is consistent with its distribution across multiple recalcitrant phases within the sample. Since both malachite/azurite and pseudomalachite contained negligible Fe (< 0.1 wt% FeO), this behaviour was likely due to the occurrence of Fe within cupro-asbolane, kolwezite, and chrysocolla (Table 3). At elevated temperature, Fe exhibited substantially higher leaching across all three DES systems, which is attributed to the breakdown of Fe-bearing minerals such as phyllosilicates and goethite, which are otherwise thermodynamically stable at lower temperatures (Majzlan et al., 2003; Robie and Waldbaum, 1970).

At low temperature (20 °C), ChCl:FA and ChCl:LA exhibited the following order of leaching Cu/Mn > Co > Ni/As > Fe. On the other hand, ChCl:OA displayed a metal leaching order of Mn > Co > Cu > As > Ni/Fe. While leaching efficiencies for most metals became similar at higher temperatures, ChCl:OA consistently achieved the highest overall metal dissolution in both high- and low-temperature conditions. However, this was accompanied by reduced efficiency and selectivity for Cu. Overall, ChCl:LA was the most effective DES for Cu and Co leaching at

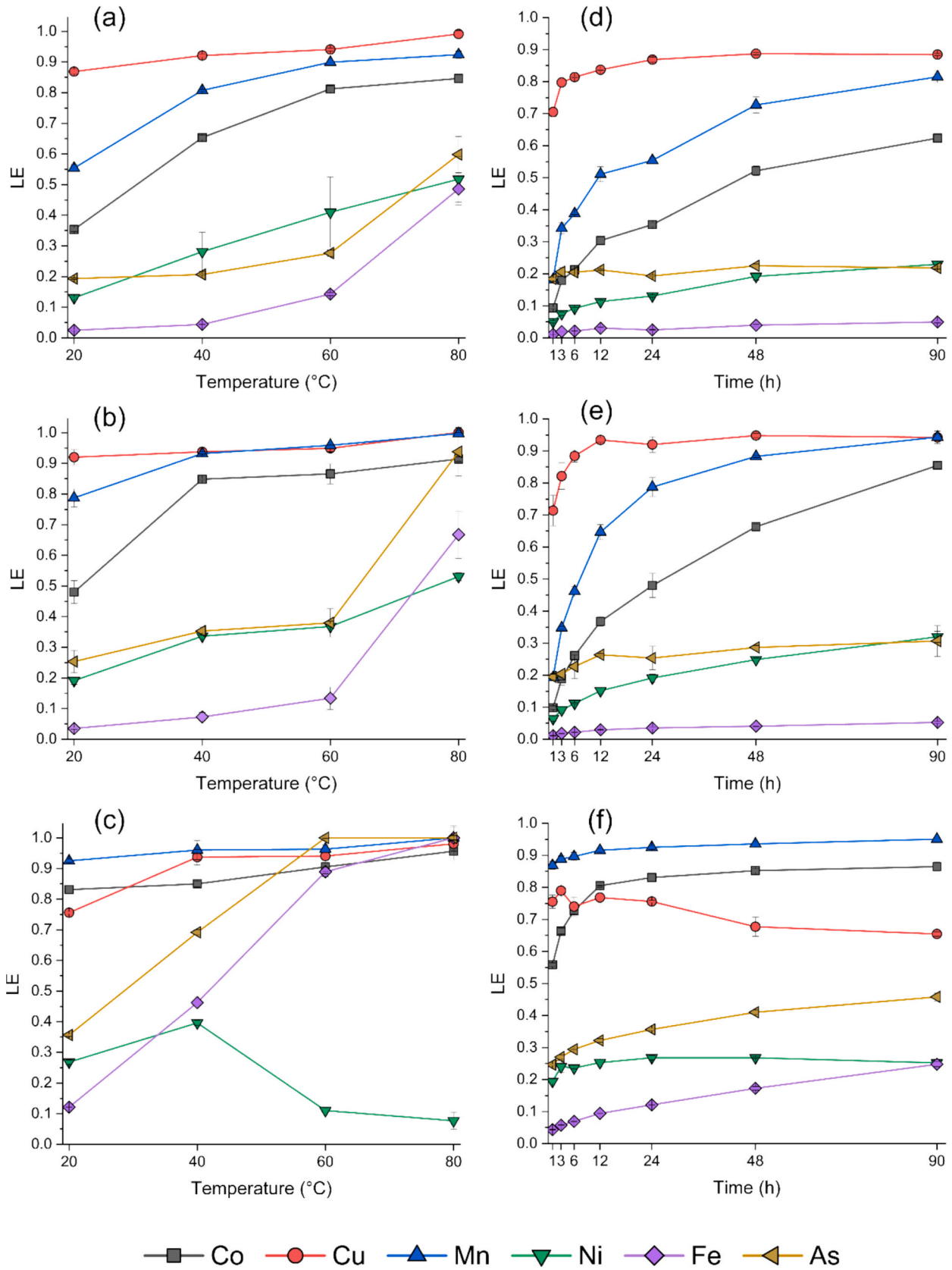

Fig. 2. Leaching efficiencies (LE) of metals/metalloids for three deep eutectic solvents. Left-hand panels (a–c) show temperature-dependent experiments (20–80 °C) for choline chloride–formic acid (ChCl:FA) (a), choline chloride–lactic acid (ChCl:LA) (b), and choline chloride–oxalic acid (ChCl:OA) (c). Right-hand panels (d–f) show time-dependent experiments (1–90 h) at 20 °C for ChCl:FA (d), ChCl:LA (e), and ChCl:OA (f).

low temperature (20 °C), with near-total Cu and Co leaching (0.94 ± 0.02 and 0.85 ± 0.01, respectively) recorded after 90 h, and low leaching of Fe (0.05 ± 0.00) (Fig. 2e; Fig. 3). ChCl:LA achieved Cu equilibria faster than ChCl:FA (~12 h vs ~ 48 h, respectively), but the slow equilibrium of Co required a long mixing time (90 h).

The leaching behaviour of 10 g/L sulfuric acid—with and without 1.5 g/L $FeSO_4$ added—was also investigated for the ore sample, to benchmark DES performance against the current industry standard (Fig. 4). The time-series plots for sulfuric acid leaching (Fig. 4a) indicate that at 20 °C, the leaching of Cu-minerals was rapid (within 1 h), but this was not the case for the Co– and Mn-minerals, even after 90 h. The addition of 1.5 g/L $FeSO_4$ (Fig. 4b) had no discernible effect on the leaching efficiency of Cu (0.96 ± 0.02 after 1 h), but significantly enhanced Co and Mn leaching. After 1 h, Co reached 0.79 ± 0.01 compared to 0.18 ± 0.01 for H_2SO_4 without $FeSO_4$. Manganese leaching was similarly rapid, whereas Fe dissolution remained largely unchanged. These results indicate that the Fe^{2+} reducing agent (within the $FeSO_4$) promoted more effective dissolution of Co– and Mn-bearing minerals.

Under identical conditions, H_2SO_4 exhibited faster Cu leaching kinetics than all three DESs. However, after 12 h, Cu leaching efficiencies reached similar levels for all solvents, except ChCl:OA. For Co, H_2SO_4 yielded higher leaching efficiency than ChCl:FA (0.76 ± 0.06 versus 0.62 ± 0.01 at 90 h) but was outperformed by both ChCl:OA and ChCl:LA, which reached 0.86 ± 0.01 and 0.85 ± 0.01, respectively (Fig. 3). Ferrous sulfate-dosed H_2SO_4 demonstrated the fastest initial leaching kinetics for Cu, Co, and Mn. However, after 90 h, ChCl:OA and ChCl:LA shared comparable leaching efficiencies for Co (Fig. 3). Copper leaching efficiencies in ChCl:OA were substantially lower than those in ferrous sulfate-dosed H_2SO_4 and ChCl:LA. In contrast, ChCl:LA exhibited nearly complete Cu dissolution and sustained high Co leaching efficiency (> 0.85), while maintaining low Fe leaching efficiency (0.05) relative to the ferrous sulfate system (0.08). This suggests that ChCl:LA offers superior selectivity for Cu and Co at 20 °C over extended durations.

XPS was used to examine the surface composition of the leached residues extracted from ChCl:OA, ChCl:LA and ChCl:FA after 1 h, 6 h, and 24 h. Cobalt and Mn were below the XPS detection limit (0.05 ± 0.02 at. %). This absence of Co and Mn detected by XPS is consistent with their partial dissolution under the investigated conditions. XPS is unlikely to reflect the bulk composition of the samples, because its surface sensitivity means that only the outermost atomic layers are analysed. After 24 h, the Cu 2p spectra could only be resolved for the ChCl:FA residue, indicating the extent of Cu dissolution with ChCl:LA and ChCl:OA (Fig. S3). The Fe 2p spectra revealed a single oxidation state of Fe, likely Fe(III), in the leached residues (Pratt et al., 1994; Grosvenor et al., 2004). The O 1 s spectra showed a metal–oxygen (M−O) peak at *ca.* 529 eV and an oxygen–organic carbon peak at *ca.* 532 eV (Fig. S4). Significant changes in the ratio of these two components are indicative of a chemical change in the sample (Fig. S4) (Henderson et al., 2025). In the ChCl:OA leached residue, the ratio of the M−O peak to the organic carbon peak was higher (1:7) than in the ChCl:FA (1:12) and ChCl:LA (1:20) residues. This suggests that a greater proportion of M−O species are present after leaching with ChCl:OA, indicating a higher degree of surface chemical reaction compared to the other DESs. The greater extent of reaction helps to explain the overall higher metal leaching efficiency with ChCl:OA. The organic carbon signal primarily reflected background surface contamination and served here as a reference for evaluating relative surface composition changes.

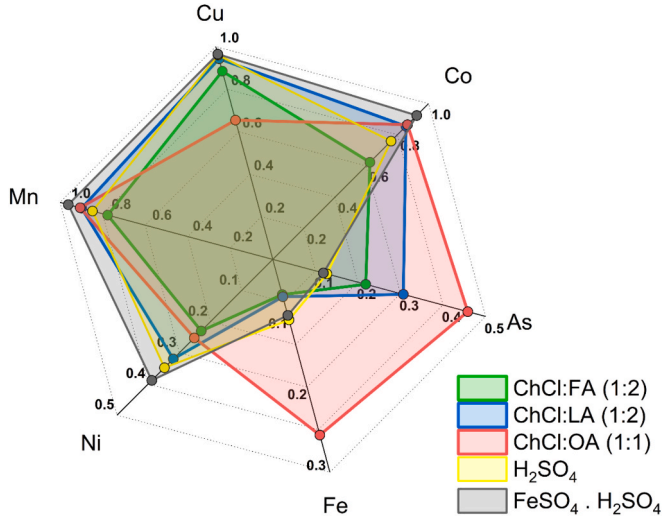

Fig. 3. Comparison of ChCl:OA (red), ChCl:FA (blue), ChCl:LA (green), H_2SO_4 (10 g/L) (yellow), 1.5 g/L ferrous sulfate-dosed H_2SO_4 (grey) leaching efficiencies after 90 h at 20 °C. (For interpretation of the references to colour in this figure legend, the reader is referred to the web version of this article.)

3.3. Leaching mechanism

Metal dissolution increased with temperature for all DESs tested (Fig. 2a–c). Nickel did not follow this behaviour in ChCl:OA, particularly at higher temperatures (>40 °C). The speciation of Ni in ChCl-DES stands out because instead of forming tetrachloro complexes, it is coordinated by oxygen donors (Hartley et al., 2014). In the case of oxalic acid DES, Ni may have coordinated to oxalate forming an insoluble precipitate, which appears enhanced at higher temperature (Asadrokht and Zakeri, 2022; Pateli et al., 2020). Increasing the leaching temperature reduced the viscosity of the DES, which enhanced its ability to penetrate micropores within the ore, and increased the kinetic energy of the DES, leading to stronger interactions with the mineral lattice. While this is usually beneficial for target metal leaching, it also caused non-selective leaching of Fe and As, which would pose challenges for effectively isolating Co and Cu and for treating post-leachate solutions. Also, DESs are susceptible to esterification and thermal decomposition at elevated temperatures, which can both lower their leaching efficacy and potentially result in the formation of hazardous byproducts (Peeters et al., 2022; Pinho et al., 2024; Rodriguez et al., 2019).

Rapid Cu leaching in all systems was likely due to proton-driven dissolution of malachite and pseudomalachite (Table 2; Table 3). The slower leaching kinetics of Co and Mn were consistent with their abundance in cupro-asbolane. Since Mn in cupro-asbolane is tetravalent, which is a relatively insoluble Mn valence state compared to its trivalent form, it is considered to break down predominantly via reductive dissolution (Moro et al., 2023; Sinha & Purcell, 2019). Such dissolution could, in turn, lead to the liberation of Co and Cu held within cupro-asbolane. Therefore, it can be suggested that Co was released via the reductive dissolution of cupro-asbolane by the DES HBD-ligands and Fe^{2+}.

Stronger acid systems (ChCl:OA and H_2SO_4, and ferrous-H_2SO_4) achieved high Cu and Co leaching efficiencies but were non-selective, facilitating greater Fe dissolution compared to ChCl:FA and ChCl:LA, particularly above 20 °C (Fig. 3). These systems promoted greater proton-driven dissolution of relatively insoluble Fe-bearing gangue minerals, such as chlorite and biotite (Table 2). In contrast, ChCl:FA and ChCl:LA showed enhanced selectivity. This may be due to the higher pKa values of lactic and formic acids (Table S3), which decreased proton-driven gangue dissolution, along with their milder redox potentials compared to the oxalic acid in ChCl:OA (Table S4). Oxalic acid is capable of reductive dissolution Mn(IV) and Fe(III) minerals by ligand-assisted electron transfer (Panias et al., 1996; Sinha and Purcell, 2019). This is because oxalic acid is a strong reducing agent, $pE_0 = -10.05$ at 25 °C (Sobianowska-Turek et al., 2014). In contrast, formic and lactic acids are milder reductants (Table S4), less effective at reducing more thermodynamically stable Fe(III)OOH, but effective at reducing Mn(IV) and Co(III) minerals—which behave as strong oxidisers (Pateli et al.,

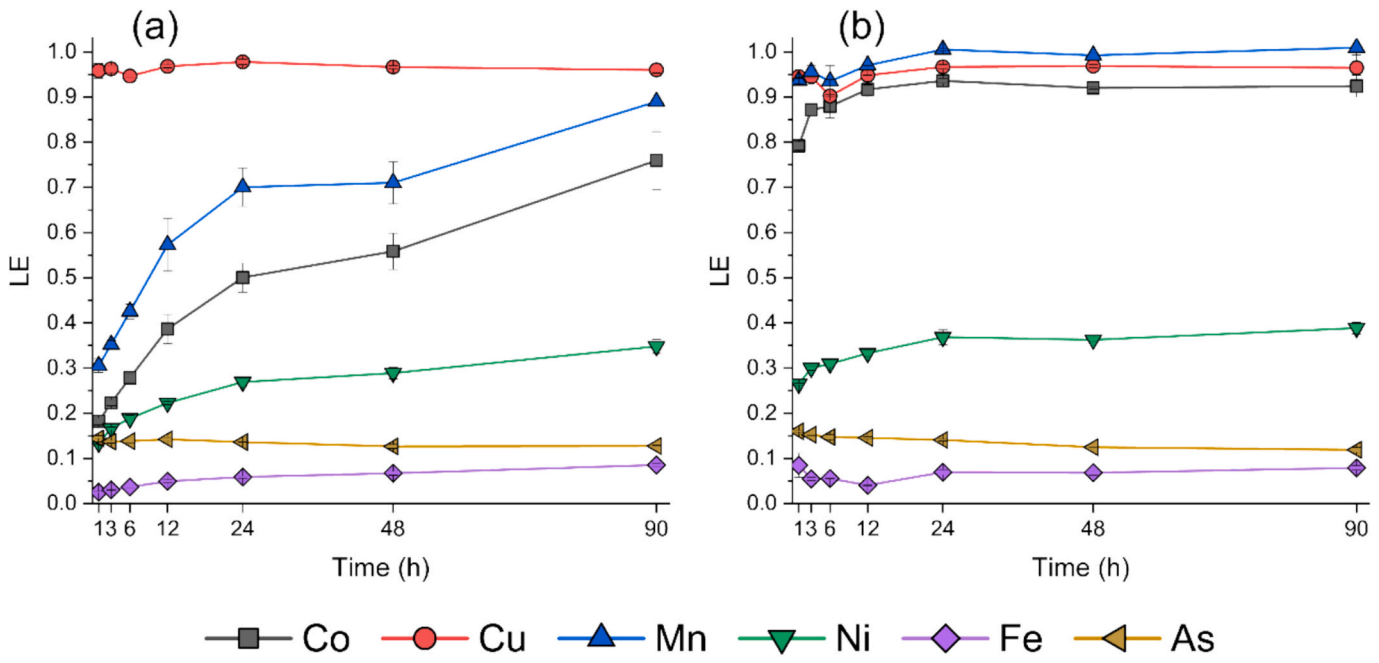

Fig. 4. Leaching efficiencies (LE) of metals/metalloids in time-dependent experiments (1–90 h) at 20 °C for H_2SO_4 (10 g/L) (a), and ferrous sulfate dosed (1.5 g/L) H_2SO_4 (b).

2020)—thus selectively releasing Co and Cu versus Fe.

It is widely agreed that, in addition to their different pKa values, the coordinating ability of the HBD ligand makes an important contribution to metal dissolution performance of the DES (Mishra et al., 2023; Pateli et al., 2020). Formic acid forms the weakest coordination complexes because of its monodentate carboxyl group. Although lactic and oxalic acids are chelating agents that form stronger complexes than formic acid, oxalic acid forms even stronger complexes than lactic acid due to its dicarboxylic nature. The leaching efficiencies of Co, Mn, As, and Fe at 20°C followed the order ChCl:FA < ChCl:LA < ChCl:OA (Fig. 3), whereas acidity followed the order ChCl:LA < ChCl:FA < ChCl:OA (Table S3). This suggests that the additional ligands in the chelating HBDs contributed to the enhanced metal dissolution performance exhibited by ChCl:OA and ChCl:LA.

Our findings correspond to observations by Mishra et al. (2023) that CuO dissolution was lower in ChCl:OA compared to ChCl:FA. Low Cu leaching efficiency in ChCl:OA could be due to the formation of insoluble Cu(II)–oxalate following dissolution of Cu minerals. This hypothesis is in accordance with the Irving–Williams Series, which ranks the stability of high-spin divalent metal complexes as Mn < Fe < Co < Ni < Cu > Zn, independent of ligand (Irving and Williams, 1948). The stability constants for Cu(II)–oxalate ($\log K_1 = 6.16$; $\log K_2 = 8.5$) are significantly greater than those for other divalent metal cations, indicating a strong affinity of Cu(II)–oxalate in systems containing disassociated oxalic acid (Lange and Speight, 2005). This high complexation tendency, combined with elevated Cu^{2+} concentrations in solution, probably resulted in the precipitation of Cu(II)–oxalate in the ChCl:OA system (Pateli et al., 2020). The use of ChCl:OA at 20 °C should be restricted to leaching durations of < 24 h to achieve selectivity of Cu and Co over Fe. In contrast, other HBD ligands form weaker complexes with Cu^{2+} (e.g., Cu(II)–lactate, $\log K_1 = 3.02$ (Lange and Speight, 2005), which are more labile and facilitate ligand exchange with the abundant chloride anions in the DES (Pateli et al., 2020). Despite the greater acidity, stronger coordinating ability, and greater reduction potential of ChCl:OA, the relatively milder conditions of ChCl:LA and ChCl:FA enabled higher Cu solubility during prolonged leaching.

3.4. Environmental and industrial implications

ChCl:LA and ChCl:OA demonstrated comparable Cu and Co leaching performance to the conventional industrial sulfuric acid-based hydrometallurgical approach. However, after 90 h, Co leaching efficiency with ChCl:FA was lower than that achieved by H_2SO_4 over the same period. In contrast, ChCl:LA and ChCl:OA exhibited significantly higher Co leaching efficiency than both ChCl:FA and H_2SO_4. Sodium metabisulfite (SMBS) is a commonly used reducing agent in Cu-Co hydrometallurgy, but its application is restricted by environmental and health concerns related to SO_2 emissions (Ferron, 2008). Cobalt leaching efficiencies with SMBS rarely exceed 80 % and excessive SO_2 emissions can result in penalties (Santoro et al., 2019). In contrast, ChCl:LA and ChCl:OA achieved high Co leaching efficiencies (85 % and 86 %, respectively) and avoided SO_2 emissions.

More generally, the use of H_2SO_4 in hydrometallurgy raises important concerns associated with its safe handling and environmental impacts due to its strong acidity and low biodegradability (Hyun et al., 2020; Shin et al., 2018). In contrast, DES exhibit several favourable properties, including low vapour pressure, potentially low environmental toxicity and strong ability to biodegrade (Radošević et al., 2015). Given that they are non-aqueous, DESs also offer another potential benefit by eliminating the need for water for their synthesis. This makes them highly suitable for both existing mining locations where water is scarce, but also could unlock a new paradigm of metal recovery from the vast number of currently unconventional small and/or remote mineral deposits, where water access is lacking (Binnemans and Jones, 2017).

Global demand for sulfuric acid is approximately 250 million tonnes/year and is projected to increase to 400 million tonnes/year by 2040. This growth could lead to an annual supply shortfall of 100–320 million tonnes (Maslin et al., 2022). Sulfuric acid is mainly produced through the desulfurisation of fossil fuels, and as the world shifts away from fossil fuels, concerns are being raised about the supply of cheap, sustainable sulfuric acid (Maslin et al., 2022). Greater mining of sulfides and elemental sulfur could address a potential supply shortfall, but at a significant environmental cost. Therefore, limiting the use of and reducing the demand for sulfuric acid might be the best option (Maslin et al., 2022). Our results demonstrate that sulfuric acid could be

substituted by DESs, unlocking a more sustainable future for the mining industry.

A solid–liquid ratio of 1:20 was used in this study to ensure a sufficient excess of DES, preventing external mass-transfer limitations and enabling comparison with previous DES-based systems that typically employ this ratio. However, such a high dilution may be uneconomic at industrial scale, where solid–liquid ratios of 1:3.5–10 are more common with conventional solvents. The inherently high viscosity of DESs may nevertheless justify the use of ratios closer to 1:20, or alternatively necessitate mild heating (or other viscosity-reduction strategies) when lower ratios are applied.

Furthermore, although DESs are considered to be low-cost compared with ionic liquids (Wang et al., 2025), they are currently substantially greater than sulfuric acid and ferrous dosed sulfuric acid (Table S9). For adoption at large-scale DES reuse is therefore vital both economically and environmentally (Svärd et al., 2024).

Whilst good performance for target metal leaching was recorded herein for the chosen DESs, further research is required to understand other components of the metal refining flowsheet. Namely, the high viscosity, non-aqueous nature, and organic acid content will affect steps like chemical precipitation, solvent extraction (SX), and electrowinning (EW). For example, the use of additives to reduce viscosity or induce selective metal precipitation may diminish its leaching efficiency in subsequent cycles and potentially contaminate recovered metals (Svärd et al., 2024). Although proof-of-concept EW has been demonstrated for ChCl–ethylene glycol and ChCl–urea systems, EW from ChCl:FA, ChCl:LA, or ChCl:OA has not, to our knowledge, yet been established (Chiorcea-Paquim and Brett, 2025). Furthermore, redox processes may degrade organic components and generate hazardous by-products during EW (Svärd et al., 2024).

Within leaching applications, the chemical reactions between the metal oxides and the HBD ligands likely result in the consumption of protons as well as the oxidation and precipitation of organic anions. These reactions, along with the production of water from the protonation of oxides, raise concerns surrounding the watering down of DES properties across leaching cycles and suggest a limit to their long-term reusability (Svärd et al., 2024).

4. Conclusions

Developing sustainable and efficient metal extraction processes is a priority to meet the escalating demand for Cu and Co and to tackle the environmental challenges associated with current mining practices. Herein, we have investigated three different Type III DES (ChCl–carboxylic acid): ChCl–formic acid (1:2), ChCl–lactic acid (1:2), and ChCl–oxalic acid (1:1), as a novel approach to potentially improve the cost, environmental and human health impacts of such activity. The following can be concluded:

- Mineralogical analyses using QEMSCAN® showed that the dominant Cu phases were malachite (2.6 area%), chrysocolla (1.8 area%), pseudomalachite (0.7 area%), and cupro-asbolane (0.7 area%). Cupro-asbolane was the most abundant Co-bearing phase in the sample, but low concentrations of kolwezite and heterogenite were also detected (0.1 area% and $<$ 0.1 area%, respectively). EPMA analysis of these phases confirmed malachite and pseudomalachite as the most abundant Cu phases, while chrysocolla and cupro-asbolane contained lower Cu concentrations. High Co concentrations were recorded in heterogenite (48.7 wt%), followed by kolwezite (44.8 wt%) and cupro-asbolane (7.74 wt%). These results highlight the substantial diversity of metal deportment in Cu ore, with both Cu and Co present in multiple minerals of interest. This was further corroborated by a BCR sequential extraction, which showed that Cu and Co were predominantly present in both exchangeable and reducible phases, suggesting that an acidic solvent, but also one that acts as a reducing agent, would be required for their effective leaching.
- Leaching of the Cu ore at 20 °C using the three DES formulations proceeded more slowly than at higher temperatures, but with improved selectivity, with minimal dissolution of Fe and As. Among the DESs tested, ChCl:LA demonstrated the best overall performance after 90 h, achieving Cu, Co, and Fe leaching efficiencies of 0.94, 0.85, and 0.05, respectively. ChCl:OA was highly effective at leaching both Cu and Co after only 1 h; however, with longer leaching durations, Cu recovery decreased, and substantial leaching of gangue minerals, including Fe-bearing minerals, occurred. In contrast, both ChCl:LA and ChCl:FA were relatively selective for Cu and Co at such temperatures. At 80 °C, near-total dissolution of Cu and Co was achieved by all DESs tested; however, this process was relatively non-selective, resulting in substantial leaching of non-target metals.
- Leaching of the ore using the conventional H_2SO_4 process was more rapid than all DESs tested for Cu leaching, but the opposite was observed for Co in ChCl:LA and ChCl:OA, which exhibited higher Co efficiencies. Notably, ChCl:LA also maintained high Cu leaching performance over extended durations, whilst ChCl:OA did not.
- When H_2SO_4 was paired with ferrous sulfate, the ferrous acid dissolved Cu and Co with high efficiency (0.96 and 0.92, respectively). The rate of Co dissolution was higher for sulfuric acid dosed with ferrous sulfate compared to all the DESs, which might be attributed to the higher viscosity of the latter and the lower pKa of sulfuric acid. However, at low temperature (20 °C), prolonged leaching over 90 h revealed that ChCl:LA offered superior selectivity for Cu and Co. It maintained comparable leaching efficiencies for both Cu and Co while reducing Fe dissolution by almost a half, which is beneficial for minimising Fe impurities in the final concentrate.

Overall, our results indicate that DESs are a highly promising alternative to conventional sulfuric acid-based leaching of Cu ore. Within this, ChCl:LA exhibited particularly high performance and selectivity for Cu and Co leaching, but with low Fe dissolution, with such selectivity enhanced at lower temperatures. The DESs tested herein can therefore be concluded as exhibiting comparable performance for Cu and Co leaching to conventional sulfuric acid-based leaching, but also offer a range of highly promising environmental and human health advantages due to their low vapour pressure, biodegradability, potentially low environmental toxicity, and unique non-aqueous properties. They therefore pose as a highly promising new route for the combined leaching of Cu and Co from SSH Cu ore. Further work is required to examine its industrial viability, including upscaled tests, exploration of solvent extraction and DES reuse considerations and ecological impact assessment.

CRediT authorship contribution statement

Rupert Heathcote: . **William Nash:** Writing – review & editing, Supervision, Methodology. **Arthur Graf:** Writing – original draft, Visualization, Software, Formal analysis. **Karen A. Hudson-Edwards:** Writing – review & editing, Supervision. **Rich Crane:** Writing – review & editing, Supervision, Project administration, Methodology, Funding acquisition.

Declaration of competing interest

The authors declare that they have no known competing financial interests or personal relationships that could have appeared to influence the work reported in this paper.

Acknowledgments

This study was funded by the Engineering and Physical Sciences Research Council Doctoral Training Partnership (EPSRC DTP) PhD

studentship (EP/T518049/1). The authors would like to thank Mintek for providing the geological sample. The experiments were performed at Camborne School of Mines (CSM) laboratory facilities. The authors thank CSM technical services staff including Gavyn Rollinson for QEMSCAN® analysis of the sample block and Sharon Uren for her assistance with milled sample digestion. The authors thank Ursula Leyland for her assistance with laboratory experiments. The authors also express thanks to Stuart Kerns, Jon Wade, Andrew Matzen and NERC for organising and funding the Advanced Training Course in Quantitative X-ray Microanalysis at the University of Oxford. XPS analysis was undertaken at the EPSRC National Facility for XPS (HarwellXPS), operated by Cardiff University and UCL, under Contract No. PR16195.

Appendix A. Supplementary material

Supplementary data to this article can be found online at https://doi.org/10.1016/j.mineng.2025.109990.

Data availability

Data supporting this study will be available from ORE Repository at https://ore.exeter.ac.uk/Doctoral_College_Theses_and_Dissertations/groups.

References

Abbott, A., Frisch, G., 2013. Element Recovery and Sustainability – Ionometallurgy: Processing of Metals using Ionic Liquids, in: Hunt, A. (Ed.), . Royal Society of Chemistry, pp. 59–79.

Abbott, A.P., Capper, G., Davies, D.L., Rasheed, R.K., Shikotra, P., 2005. Selective extraction of metals from mixed oxide matrixes using choline-based ionic liquids. Inorg. Chem. 44, 6497–6499. https://doi.org/10.1021/ic0505450.

Abbott, A.P., Capper, G., Davies, D.L., Rasheed, R.K., Tambyrajah, V., 2003. Novel solvent properties of choline chloride/urea mixtures. Chem. Commun. 70–71. https://doi.org/10.1039/b210714g.

Abranches, D.O., Coutinho, J.A.P., 2023. Everything you wanted to know about deep eutectic solvents but were afraid to be told. Annu. Rev. Chem. Biomol. Eng. 2023 (14), 2023. https://doi.org/10.1146/annurev-chembioeng.

Anggara, S., Bevan, F., Harris, R.C., Hartley, J.M., Frisch, G., Jenkin, G.R.T., Abbott, A.P., 2019. Direct extraction of copper from copper sulfide minerals using deep eutectic solvents. Green Chem. 21, 6502–6512. https://doi.org/10.1039/c9gc03213d.

Aragón-Tobar, C.F., Endara, D., de la Torre, E., 2024. Dissolution of metals (Cu, Fe, Pb, and Zn) from different metal-bearing species (Sulfides, Oxides, and Sulfates) using three deep eutectic solvents based on choline chloride. Molecules 29. https://doi.org/10.3390/molecules29020290.

Asadrokht, M., Zakeri, A., 2022. Chemo-physical concentration of a low-grade nickel laterite ore. Miner. Eng. 178. https://doi.org/10.1016/j.mineng.2022.107398.

Binnemans, K., Jones, P.T., 2023a. Methanesulfonic acid (MSA) in hydrometallurgy. J. Sustain. Metall. https://doi.org/10.1007/s40831-022-00641-6.

Binnemans, K., Jones, P.T., 2023b. The twelve principles of circular hydrometallurgy. J. Sustain. Metall. 9, 1–25. https://doi.org/10.1007/s40831-022-00636-3.

Binnemans, K., Jones, P.T., 2017. Solvometallurgy: an emerging branch of extractive metallurgy. J. Sustain. Metall. https://doi.org/10.1007/s40831-017-0128-2.

Brusselen, V., Herck, V., Avonts, D, Kayembe-Kitenge, T, Musa Obadia, P, Kyanika Wa Mukoma, D, Banza, C, Nkulu, L., Obadia, M., Van Brusselen, D., Kayembe-Kitenge, Tony, Mbuyi-Musanzayi, S., Kasole, T.L., Ngombe, L.K., Musa Obadia, Paul, Kyanika Wa Mukoma, Daniel, Van Herck, K., Avonts, Dirk, Devriendt, K., Smolders, E., Banza, Célestin, Nemery, B., 2020. Metal mining and birth defects: a case-control study in Lubumbashi, Democratic Republic of the Congo, Articles Lancet Planet Health.

Bystrzanowska, M., Tobiszewski, M., 2021. Assessment and design of greener deep eutectic solvents – a multicriteria decision analysis. J. Mol. Liq. 321. https://doi.org/10.1016/j.molliq.2020.114878.

Carlesi, C., Harris, R.C., Abbott, A.P., Jenkin, G.R.T., 2022. Chemical dissolution of chalcopyrite concentrate in choline chloride ethylene glycol deep eutectic solvent. Minerals 12. https://doi.org/10.3390/min12010065.

Chiorcea-Paquim, A.M., Brett, C.M.A., 2025. Electrodeposition in deep eutectic solvents: Perspectives towards advanced corrosion protection. Appl. Mater. Today 44. https://doi.org/10.1016/j.apmt.2025.102746.

Clarke, C.J., Tu, W.C., Levers, O., Bröhl, A., Hallett, J.P., 2018. Green and sustainable solvents in chemical processes. Chem. Rev. 118, 747–800. https://doi.org/10.1021/acs.chemrev.7b00571.

Crundwell, F.K., du Preez, N.B., Knights, B.D.H., 2020. Production of cobalt from copper-cobalt ores on the African Copperbelt – an overview. Miner. Eng. 156. https://doi.org/10.1016/j.mineng.2020.106450.

Decrée, S., Deloule, É., Ruffet, G., Dewaele, S., Mees, F., Marignac, C., Yans, J., de Putter, T., 2010. Geodynamic and climate controls in the formation of Mio-Pliocene world-class oxidized cobalt and manganese ores in the Katanga province DR Congo. Miner. Depos. https://doi.org/10.1007/s00126-010-0305-8.

Dehaine, Q., Tijsseling, L.T., Glass, H.J., Törmänen, T., Butcher, A.R., 2021. Geometallurgy of cobalt ores: a review. Miner. Eng. https://doi.org/10.1016/j.mineng.2020.106656.

Ferron, J.C., 2008. Sulfur dioxide a versatile reagent for the processing of cobalt oxide minerals. Aqueous Processing.

Fisher, K.G., 2011. Cobalt processing developments. 6th Southern African Base Metals Conference.

Grosvenor, A.P., Kobe, B.A., Biesinger, M.C., McIntyre, N.S., 2004. Investigation of multiplet splitting of Fe 2p XPS spectra and bonding in iron compounds. Surf. Interface Anal. 36, 1564–1574. https://doi.org/10.1002/sia.1984.

Hansen, B.B., Spittle, S., Chen, B., Poe, D., Zhang, Y., Klein, J.M., Horton, A., Adhikari, L., Zelovich, T., Doherty, B.W., Gurkan, B., Maginn, E.J., Ragauskas, A., Dadmun, M., Zawodzinski, T.A., Baker, G.A., Tuckerman, M.E., Savinell, R.F., Sangoro, J.R., 2021. Deep eutectic solvents: a review of fundamentals and applications. Chem. Rev. https://doi.org/10.1021/acs.chemrev.0c00385.

Hartley, J., Ip, C.-M., Forrest, G., Singh, K., Gurman, S., Ryder, K., Abbott, A., Frisch, G., 2014. EXAFS study into the speciation of metal salts dissolved in ionic liquids and deep eutectic solvents. Inorg. Chem. 53, 6280–6288. https://doi.org/10.1021/ic500824r.

Henderson, J.D., Payne, B.P., McIntyre, N.S., Biesinger, M.C., 2025. Enhancing oxygen spectra interpretation by calculating oxygen linked to adventitious carbon. Surf. Interface Anal. https://doi.org/10.1002/sia.7376.

Hyun, S.P., Shin, D., Moon, H.S., Han, Y.S., Ha, S., Lee, Y., Lee, E., Jung, H., Hwang, Y.S., 2020. A multidisciplinary assessment of the impact of spilled acids on geoecosystems: an overview. Environ. Sci. Pollut. Res. 27, 9803–9817. https://doi.org/10.1007/s11356-019-07586-6.

IEA, 2024. Global Critical Minerals Outlook 2024.

Igor Azeuda Ndonfack, K., Yang, Z., Zhang, J., Whattam, S.A., Xie, Y., 2024. Geology, geochemistry, and exploration of the Central African Copperbelt: a review. Int Geol Rev. https://doi.org/10.1080/00206814.2024.2426200.

Irving, H., Williams, R.J.P., 1948. Order of stability of metal complexes. Nature 162, 746–747.

Jenkin, G.R.T., Al-Bassam, A.Z.M., Harris, R.C., Abbott, A.P., Smith, D.J., Holwell, D.A., Chapman, R.J., Stanley, C.J., 2016. The application of deep eutectic solvent ionic liquids for environmentally-friendly dissolution and recovery of precious metals. Miner. Eng. 87, 18–24. https://doi.org/10.1016/j.mineng.2015.09.026.

Kalenga, J.N., 2013. Economic and Toxicological aspects of copper industry in Katanga, DR Congo. Jpn. J. Vet. Res. 61, 23–32.

Kayembe-Kitenge, T., Musa Obadia, P., Kasole Lubala, T., Mbuyi-Musanzay, S., Katoto, P., Kalenga Ilunga, G., Katshiez Nawej, C., Nkulu, B.L., Nemery, B., 2019. Incidence of congenital malformations and proximity to mining in Lubumbashi, DR Congo. Environ. Epidemiol. 3, 194. https://doi.org/10.1097/01.EE9.0000607948.37552.92.

Landa-Castro, M., Aldana-González, J., Montes de Oca-Yemha, M.G., Romero-Romo, M., Arce-Estrada, E.M., Palomar-Pardavé, M., 2020. Ni–Co alloy electrodeposition from the cathode powder of Ni-MH spent batteries leached with a deep eutectic solvent (reline). J. Alloy. Compd. 830. https://doi.org/10.1016/j.jallcom.2020.154650.

Lange, N.Adolph., Speight, J.G.., 2005. Electroyltes, Electromotive Force, and Chemical Equilibrium, in: Lange's Handbook of Chemistry. McGraw-Hill, pp. 8.89-8.103.

Lutandula, M.S., Maloba, B., 2013. Recovery of cobalt and copper through reprocessing of tailings from flotation of oxidised ores. J. Environ. Chem. Eng. 1, 1085–1090. https://doi.org/10.1016/j.jece.2013.08.025.

Majzlan, J., Grevel, K.-D., Navrotsky, A., 2003. Thermodynamics of Fe oxides: part II. enthalpies of formation and relative stability of goethite (a-FeOOH), lepidocrocite (g-FeOOH), and maghemite (g-Fe_2O_3). Am. Mineral. 88, 855–859.

Mambwe, P., Shengo, M., Kidyanyama, T., Muchez, P., Chabu, M., 2022. Geometallurgy of cobalt black ores in the katanga copperbelt (Ruashi Cu-Co Deposit): a new proposal for enhancing cobalt recovery. Minerals 12. https://doi.org/10.3390/min12030295.

Maslin, M., Van Heerde, L., Day, S., 2022. Sulfur: a potential resource crisis that could stifle green technology and threaten food security as the world decarbonises. Geogr. J. 188, 498–505. https://doi.org/10.1111/geoj.12475.

Mishra, S., Hunter, T.N., Pant, K.K., Harbottle, D., 2024. Green deep eutectic solvents (DESs) for sustainable metal recovery from thermally treated PCBs: a greener alternative to conventional methods. ChemSusChem 17. https://doi.org/10.1002/cssc.202301418.

Mishra, S., Pandey, A., Pant, K.K., Mishra, B., 2023. Investigating the effect of mono di carboxylic acids as hydrogen bond donor on solvation of copper in choline chloride-based deep eutectic solvents. J. Mol. Liq. 383. https://doi.org/10.1016/j.molliq.2023.122142.

Misra, K.C., 2000. Sediment-Hosted Stratiform Copper (SSC) deposits. In: Understanding Mineral Deposits. Springer, Netherlands, Dordrecht, pp. 539–572. https://doi.org/10.1007/978-94-011-3925-0_12.

Moro, K., Haubrich, F., Martin, M., Grimmer, M., Hoth, N., Schippers, A., 2023. Reductive leaching behaviour of manganese and cobalt phases in laterite and manganese ores. Hydrometallurgy 220. https://doi.org/10.1016/j.hydromet.2023.106101.

Muimba-Kankolongo, A., Banza Lubaba Nkulu, C., Mwitwa, J., Kampemba, F.M., Mulele Nabuyanda, M., 2022. Impacts of Trace Metals Pollution of Water, Food Crops, and Ambient Air on Population Health in Zambia and the DR Congo. J Environ Public Health 2022. https://doi.org/10.1155/2022/4515115.

Oke, E.A., Fedai, Y., Potgieter, J.H., 2025. Hydrometallurgical leaching of copper and cobalt from a copper–cobalt ore by aqueous choline chloride-based deep eutectic solvent solutions. Minerals 15, 815. https://doi.org/10.3390/min15080815.

Panias, D., Taxiarchou, M., Paspaliaris, I., Kontopoulos, A., 1996. Mechanisms of Dissolution of Iron Oxides in Aqueous Oxalic Acid Solutions. Hydrometallurgy, ELSEVIER.

Pateli, I.M., Thompson, D., Alabdullah, S.S.M., Abbott, A.P., Jenkin, G.R.T., Hartley, J. M., 2020. The effect of pH and hydrogen bond donor on the dissolution of metal oxides in deep eutectic solvents. Green Chem. 22, 5476–5486. https://doi.org/10.1039/d0gc02023k.

Peeters, N., Janssens, K., de Vos, D., Binnemans, K., Riaño, S., 2022. Choline chloride-ethylene glycol based deep-eutectic solvents as lixiviants for cobalt recovery from lithium-ion battery cathode materials: are these solvents really green in high-temperature processes? Green Chem. 24, 6685–6695. https://doi.org/10.1039/d2gc02075k.

Pinho, M.R., Lima, A.S., de Almeida Ribeiro Oliveira, G., Liao, L.M., Franceschi, E., Silva, R. da, Cardozo-Filho, L., 2024. Choline Chloride- and Organic Acids-Based Deep Eutectic Solvents: Exploring Chemical and Thermophysical Properties. J Chem Eng Data. https://doi.org/10.1021/acs.jced.3c00706.

Pratt, A.R., Muir, I.J., Nesbitt, H.W., 1994. X-ray photoelectron and Auger electron spectroscopic studies of pyrrhotite and mechanism of air oxidation. Geochim. Cosmochim. Acta.

Radošević, K., Cvjetko Bubalo, M., Gaurina Srček, V., Grgas, D., Landeka Dragičević, T., Redovniković, R.I., 2015. Evaluation of toxicity and biodegradability of choline chloride based deep eutectic solvents. Ecotoxicol. Environ. Saf. 112, 46–53. https://doi.org/10.1016/j.ecoenv.2014.09.034.

RAID, 2024. Beneath the Green: A critical look at the environmental and human costs of industrial cobalt mining in DRC.

Rauret, G., López-Sánchez, J.F., Sahuquillo, A., Rubio, R., Davidson, C., Ure, A., Quevauviller, P., 1999. Improvement of the BCR three step sequential extraction procedure prior to the certification of new sediment and soil reference materials. J. Environ. Monit. 1, 57–61. https://doi.org/10.1039/a807854h.

Riaño, S., Petranikova, M., Onghena, B., Vander Hoogerstraete, T., Banerjee, D., Foreman, M.R.S., Ekberg, C., Binnemans, K., 2017. Separation of rare earths and other valuable metals from deep-eutectic solvents: a new alternative for the recycling of used NdFeB magnets. RSC Adv. 7, 32100–32113. https://doi.org/10.1039/c7ra06540j.

Robie, R.A., Waldbaum, D.R., 1970. Thermodynamic Properties of Minerals and Related Substances at 298.15°K (25.0°C) and One Atmosphere (1.013 Bars) Pressure and at Higher Temperatures Geological Survey Bulletin 1259. Washington D.C.

Rodriguez, N., Van Den Bruinhorst, A., Kollau, L.J.B.M., Kroon, M.C., Binnemans, K., 2019. Degradation of deep-eutectic solvents based on choline chloride and carboxylic acids. ACS Sustain. Chem. Eng. 7, 11521–11528. https://doi.org/10.1021/acssuschemeng.9b01378.

Santoro, L., Tshipeng, S., Pirard, E., Bouzahzah, H., Kaniki, A., Herrington, R., 2019. Mineralogical reconciliation of cobalt recovery from the acid leaching of oxide ores from five deposits in Katanga (DRC). Miner. Eng. 137, 277–289. https://doi.org/10.1016/j.mineng.2019.02.011.

Schlesinger, M., King, M., Sole, K., Davenport, W., 2011. Extractive Metallurgy of Copper, Fifth. ed. Elsevier, Amsterdam.

Sharma, A., Lee, B.S., 2024. Toxicity test profile for deep eutectic solvents: a detailed review and future prospects. Chemosphere. https://doi.org/10.1016/j.chemosphere.2023.141097.

Shengo, M.L., Kime, M.B., Mambwe, M.P., Nyembo, T.K., 2019. A review of the beneficiation of copper-cobalt-bearing minerals in the Democratic Republic of Congo. J. Sustainable Min. https://doi.org/10.1016/j.jsm.2019.08.001.

Shin, D., Kim, Y., Moon, H.S., 2018. Fate and toxicity of spilled chemicals in groundwater and soil environment I: strong acids. Environ. Health Toxicol. 33, e2018019. https://doi.org/10.5620/eht.e2018019.

Sinha, M.K., Purcell, W., 2019. Reducing agents in the leaching of manganese ores: a comprehensive review. Hydrometallurgy 187, 168–186. https://doi.org/10.1016/j.hydromet.2019.05.021.

Smith, E.L., Abbott, A.P., Ryder, K.S., 2014. Deep eutectic solvents (DESs) and their applications. Chem. Rev. https://doi.org/10.1021/cr300162p.

Sobianowska-Turek, A., Szczepaniak, W., Zabłocka-Malicka, M., 2014. Electrochemical evaluation of manganese reducers - recovery of Mn from Zn-Mn and Zn-C battery waste. J. Power Sources 270, 668–674. https://doi.org/10.1016/j.jpowsour.2014.07.136.

Svärd, M., Ma, C., Forsberg, K., Schiavi, P.G., 2024. Addressing the Reuse of Deep Eutectic Solvents in Li-Ion Battery Recycling: Insights into Dissolution Mechanism, Metal Recovery, Regeneration and Decomposition. ChemSusChem. https://doi.org/10.1002/cssc.202400410.

Tanda, B.C., Eksteen, J.J., Oraby, E.A., 2017. An investigation into the leaching behaviour of copper oxide minerals in aqueous alkaline glycine solutions. Hydrometall. 167, 153–162. https://doi.org/10.1016/j.hydromet.2016.11.011.

Terry, B., 1983. The acid decomposition of silicate minerals part i. reactivities and modes of dissolution of silicates, Hydrometallurgy.

Thompson, D.L., Pateli, I.M., Lei, C., Jarvis, A., Abbott, A.P., Hartley, J.M., 2022. Separation of nickel from cobalt and manganese in lithium ion batteries using deep eutectic solvents. Green Chem. 24, 4877–4886. https://doi.org/10.1039/d2gc00606e.

Tran, M.K., Rodrigues, M.T.F., Kato, K., Babu, G., Ajayan, P.M., 2019. Deep eutectic solvents for cathode recycling of Li-ion batteries. Nat. Energy 4, 339–345. https://doi.org/10.1038/s41560-019-0368-4.

USGS, 2025. Mineral Commodity Summaries 2025. https://doi.org/10.3133/mcs2025.

Valenta, R.K., Kemp, D., Owen, J.R., Corder, G.D., Lèbre, 2019. Re-thinking complex orebodies: Consequences for the future world supply of copper. J Clean Prod 220, 816–826. https://doi.org/10.1016/j.jclepro.2019.02.146.

Wang, C., Zhou, Z., Zhang, X., Guo, H., Boczkaj, G., 2025. Metal extraction using deep eutectic solvents for metal recovery and environmental remediation – a review. Sep. Purif. Technol. 364. https://doi.org/10.1016/j.seppur.2025.132533.

Wang, S., Zhang, Z., Lu, Z., Xu, Z., 2020. A novel method for screening deep eutectic solvent to recycle the cathode of Li-ion batteries. Green Chem. 22, 4473–4482. https://doi.org/10.1039/d0gc00701c.